Radar Sensor Network Using A Set of New Ternary Codes: Theory and Application

Lei Xu and Qilian Liang, Senior Member, IEEE

Department of Electrical Engineering

University of Texas at Arlington

Arlington, TX 76010-0016 USA

Email: xu@wcn.uta.edu, liang@uta.edu

Abstract

In the radar sensor network (RSN), the interferences among different radar sensors can be effectively reduced when waveforms are properly designed. In this paper, we perform some theoretical studies on coexistence of phase coded waveforms in the RSN. We propose a new ternary codes–optimized punctured Zero Correlation Zone sequence-Pair Set (ZCZPS) and analyze their properties. Applying the new ternary codes and equal gain combination technique to the RSN, we study the detection performance versus different number of radar sensors under the different conditions. The simulation results show that the RSN using our optimized punctured ZCZPS performs better than the RSN using the same number of common codes such as the Gold codes, and much better than the single radar system no matter whether the Doppler shift is considered or not.

Index Terms : Zero correlation zone, optimized punctured ZCZ sequence-pair, radar sensor network, Doppler shift

1 Introduction

Much time and effort was devoted to designing the radar waveform for a single active radar. Among the existing work, Bell [1] who introduced information theory to radar waveform design, concluded that distributing energy is a good choice to better detect targets. Sowelam and Tewfik [2] applied a sequential experiment design procedure to select signal for radar target classification. In their work, each waveform selected maximizes the Kullback/Leibler information number that measures the dissimilarity between the observed target and the alternative targets in order to minimize the decision time. Recently, a network of multiple radar sensors are introduced to construct a radar sensor network (RSN)[4], in order to overcome performance degradation of single radar along with waveform optimization. In [3], Liang studied constant frequency (CF) pulse waveform design and proposed maximum-likelihood (ML) automatic target recognition (ATR) approach for both non-fluctuating and fluctuating targets in a RSN. Furthermore, RSN design based on linear frequency modulation (LFM) waveform was studied and LFM waveform design was applied to RSN with application to ATR with delay-Doppler uncertainty by Liang [5] as well.

In addition, pulse compression technique allows a radar to simultaneously achieve the energy of a long pulse and the resolution of a short pulse without the high peak power which is required by a high energy short duration pulse [6]. Pulse compression waveforms are obtained by adding frequency or phase modulation to a simple pulse. In this paper, we will study the pulse compression by phase coding. The pulse is divided into M bits of identical duration $t_b = T/M$, and each bit is assigned with a different phase value associated with each bit of a phase code. The criteria for selecting a specific code are the resolution properties of the resulting waveform (shape of the ambiguity function), and the ease with which the system can be implemented. However, Doppler resolution is very complicated, people try to find a code with a good correlation function rather than an ambiguity function. Since the high correlation sidelobes produce high range sidelobes which

could mask returns from targets in radar system, there has been considerable interest in study of reducing range sidelobe of corresponding codes in radar system. Considering the periodic codes, the m-sequences or Legendre sequences could achieve the lowest periodic autocorrelation function (ACF) of $|R_i(\tau \neq 0) = 1|$. For non-binary sequences, the Golomb codes [7] are a kind of two-valued (biphase) perfect codes which obtain zero periodic ACF but result in large mismatch power loss. The Ipatov code [8] shows a way of designing code pairs with perfect periodic autocorrelation (the cross correlation of the code pair) and minimal mismatch loss, but its reference code and construction method are complicated. Zero periodic autocorrelation function for all nonzero shifts could be obtained by polyphase codes, such as Frank and Zadoff codes, but the more complicated constructing methods and implementation cost are required. In addition to these well-known codes, by suffering a small S/N loss, the authors [9] present several binary pulse compression codes to greatly reduce sidelobes. In [10], pulse compression using a digital-analog hybrid technique is studied to achieve very low range sidelobes for potential application to spaceborne rain radar. Tanner et al.[11] uses time-domain weighting of the transmitted pulse to achieve a range sidelobe level of -55 dB or better in flight tests. Nevertheless, all the above work have their own disadvantages, such as the large mismatch power loss for Golomb codes, the high energy of reference code and complicated construction method for Ipatov codes and so on. It is also known that for both binary and non-binary sequences in the periodic sequence field, the sequences can not obtain ideal impulsive autocorrelation function (ACF) and ideal zero cross-correlation functions (CCF) simultaneously although ideal CCFs could be achieved alone. Since the ACF and CCF have to be limited by certain bounds, such as Welch bound [12], Sidelnikov bound [13], Sarwate bound [14], Levenshtein bound [15], etc. As a reulst, the concept of Zero Correlation Zone (ZCZ) [16][17][18] during which ideal impulsive autocorrelation function and ideal zero cross-correlation functions could be achieved simultaneously is proposed to overcome the above problems.

In this paper, we theoretically study RSN design based on phase coded waveforms. Motivated by the concept of ZCZ, we propose a set of new ternary codes– optimized punctured ZCZ sequence-Pair Set (ZCZPS) and apply them as the phase coded waveforms to RSN. The optimized punctured ZCZ sequence-Pair Set could reach zero autocorrelation sidelobe and zero mutual cross correlation values during zero correlation zone. We perform studies on the codes' properties, especially their cross correlation properties. We also simulate and analyze the target detection performance of RSN using different number of radar sensors under the different conditions of Doppler shift and time delay among transmit radar sensors. Finally, the simulation results show that RSN using the optimized punctured ZCZ sequence-pairs is superior to RSN using the same number of Gold codes, and much better than the single radar system, in terms of probability of miss and false alarm detection.

The rest of the paper is organized as following. In Section 2, we study the coexistence of phase coded waveforms in a RSN. In Section 3, we provide a ternary codes–optimized punctured ZCZ sequence-pair set and study their properties. In Section 4, we simulate the target detection performance of RSN versus different number of radars under the different conditions of Doppler shift time delay among transmit radar sensors. In Section 5, brief conclusions are drawn on RSN using our optimized punctured ZCZPS.

2 COEXISTENCE OF PHASE CODED WAVEFORMS IN RSN

2.1 Orthogonal Phase Coded Waveforms Coexist in RSN

First of all, we express the phase coded waveform as

$$x(t) = \sum_{m=0}^{M-1} x^{(m)}(t - mt_b) \tag{1}$$

Here, $x^{(m)}(t)$ is one bit of duration t_b and $T = Mt_b$ is the period of the waveform.

Each bit is phase modulated by the phase code $\beta^{(m)}$ of length M:

$$x^{(m)}(t) = \begin{cases} exp(j2\pi\beta^{(m)}t) & 0 \le t \le t_b \\ 0 & \text{elsewhere} \end{cases} \tag{2}$$

For $t > T$ or $t < 0$ (within the duration of the waveform), the periodicity implies that the complex envelope of the transmitted signal $x(t)$ obeys

$$x(t) = x(t + nT), \quad n = 0, \pm 1, \pm 2, ... \tag{3}$$

We assume that there are N radars working together in a self-organizing fashion in our RSN. The ith radar sensor transmits a waveform as

$$x_i(t) = \sum_{m=0}^{M-1} x_i^{(m)}(t - nt_b) = \sum_{m=0}^{M-1} exp(j2\pi\beta_i^{(m)}(t - mt_b)) \tag{4}$$

The cross correlation between $x_i(t)$ and $x_j(t)$ could be expressed as:

$$\begin{aligned} & R(\tau) = R(rt_b) = \frac{1}{T}\int_{-T/2}^{T/2} x_i(t)x_j^*(t-\tau)dt \qquad (5) \\ = & \sum_{m=0}^{M-1}\int_{-T/2+mt_b}^{-T/2+(m+1)t_b} exp[j2\pi\beta_i^{(m+1)}(t-(m+1)t_b)]exp^*[j2\pi\beta_j^{(M-r+m+1)}(t-(M-r+n+1)t_b)]dt \\ = & \frac{1}{M}\sum_{m=0}^{M-1} exp[j2\pi[\beta_j^{(M-r+m+1)}(Mt_b - rt_b + \frac{T}{2} + \frac{t_b}{2}) + \beta_i^{(m+1)}(-\frac{T}{2} - \frac{t_b}{2})]] \\ & sinc[t_b(\beta_i^{(m+1)} - \beta_j^{(M-r+m+1)})] \end{aligned}$$

In order to reduce the interference of different waveforms, we try to make $R(\tau)$ as small as possible when $i \neq j$. Observing the equation (5), if $\pi t_b(\beta_i^{(m+1)} - \beta_j^{(M-r+m+1)}) = k\pi, k = 1, 2, 3...$, then $R(\tau) = 0$. This result is used in the latter part of the paper. It is also easy to see that when $i = j$ and $\tau = 0$, then $sinc[t_b(\beta_i^{(m+1)} - \beta_j^{(M-r+m+1)})] = 1$ and $R(\tau)$ could be normalized as 1, which is the desirable situation in a RSN.

The orthogonal waveforms have optimized correlation property which satisfies the above con-

dition and could be expressed as

$$\frac{1}{T}\int_{-T/2}^{T/2} x_i(t)x_j^*(t-\tau)dt = \begin{cases} 1 & i=j \text{ and } \tau=0 \\ 0 & i\neq j \text{ or } \tau\neq 0 \end{cases} \tag{6}$$

As a result, orthogonal phase coded waveforms, which could minimize or remove the interference from one waveform to the other, can work well in the RSN simultaneously.

2.2 The Ambiguity Function of Phase Coded Waveforms in RSN

The effect of Doppler shift also has to be considered in the RSN. Ambiguity function (AF) [6] generally identified with Woodward [19][20] is usually used to succinctly characterize the behavior of a waveform paired with its matched filter, so it is an analytical tool for waveform design especially there are time delay and Doppler shift ambiguity.

PAF (Periodic Ambiguity Function) was introduced by Levanon [21] as an extension of the periodic autocorrelation for Doppler shift. And the single-periodic complex envelope is expressed as:

$$A(\tau, F_D) \equiv |\frac{1}{T}\int_{-T/2}^{T/2} x(t+\frac{\tau}{2})e^{j2\pi F_D t}x^*(t-\frac{\tau}{2})dt| \equiv |\hat{A}(\tau, F_D)| \tag{7}$$

Where τ is the time delay, T is one period of the signal and F_D is the Doppler shift.

Accordingly, we derive the single-periodic ambiguity function of phase coded waveform

$$\begin{aligned} & A(\tau, F_D) \\ = \; & |\frac{1}{T}\int_{-\frac{T}{2}}^{\frac{T}{2}} x(t)exp(j2\pi F_D t)x^*(t-\tau)dt| \\ = \; & |\frac{1}{T}\sum_{m=0}^{M-1}\int_{-\frac{T}{2}+mt_b}^{-\frac{T}{2}+(m+1)t_b} exp[j2\pi\beta^{(m+1)}(t-(m+1)t_b)]exp^*[j2\pi\beta^{(M-r+m+1)}(t-(M-r+m+1))] \\ & exp(j2\pi F_D t)dt| \\ = \; & |\frac{1}{M}\sum_{m=0}^{M-1} exp[j2\pi[\beta^{(M-r+m+1)}[(M-r)t_b+\frac{t_b}{2}+\frac{T}{2}]+\beta^{(m+1)}(-\frac{t_b}{2}-\frac{T}{2})+F_D(-\frac{T}{2}+(m+1)t_b)] \\ & sinc[t_b(\beta^{(m)}-\beta^{(m-r)}+F_D)]| \end{aligned} \tag{8}$$

According to equation (8), if $\pi t_b(\beta^{(m)}-\beta^{(m-r)}+F_D)=k\pi, k=1,2,3...$, the amplitude of ambiguity function is zero. Taken the previous result into account that "when $\pi t_b(\beta_i^{(m+1)}-\beta_j^{(M-r+m+1)})=k\pi, k=1,2,3...$, then $R(\tau)=0$", we achieve that "$A(\tau,F_D)=0$, when $F_D=\frac{k}{t_b}, k=0,1,2...$".

Furthermore, we extend the idea of single-periodic ambiguity to the RSN. In the RSN, all the radar sensors transmit signals, so the ith radar sensor not only receives its own back-scattered waveform, but also scattered signals generated by other radars which caused interference to the ith radar sensor. Assuming that all the transmit radar sensors transmit the signal simultaneously so that there are no time delay among the transmit radar sensors $t_1=t_2=...=t_N=0$, we study the interferences from all the other $N-1$ radars ($j\neq i$). In addition, there is time delay $\tau=mt_b$ for the matched filer corresponding to the transmitting radar i, the ambiguity function of radar i with phase coded waveform could be expressed as

$$\begin{aligned} & A_i(\tau,F_{D_1},...,F_{D_N}) \qquad (9)\\ = & |\sum_{j=1}^{N}\frac{1}{T}\int_{-\frac{T}{2}}^{\frac{T}{2}} x_j(t)exp(j2\pi F_{D_i}t)x_i^*(t-\tau)dt| \\ = & |\frac{1}{M}\sum_{j=1}^{N}\sum_{m=0}^{M-1} exp[j2\pi[\beta_i^{(M-r+m+1)}[(M-r+\frac{1}{2})t_b+\frac{T}{2}]+\beta_j^{(m+1)}(-\frac{t_b}{2}+\frac{T}{2})+F_{D_j}[-\frac{T}{2}+(m+1)t_b]]] \\ & sinc[t_b(\beta_j^{(m+1)}-\beta_i^{(M-r+m+1)}+F_{D_j})]| \end{aligned}$$

Here, $0<i\leq N$ and $\tau=rt_b$. The equation (9) consists of two parts: useful signal(reflected signal from the transmitting radar i waveform), the $j=i$ part in (9); and the interferences from other $N-1$ radar waveforms, the $j\neq i$ part in (9).

3 Optimized Punctured ZCZ Sequence-Pair Set

In this section, we provide a set of ternary codes which satisfy the requirements in the above section and could be used as phase coded waveforms in RSN.

Zero correlation zone (ZCZ) is a new concept provided by Fan [16][18] [22] [23] in which both autocorrelation and cross correlation sidelobes are zero while the time delay is kept within the Zero Correlation Zone instead of the whole period of time domain. Matsufuji and Torii have provided some methods of constructing ZCZ sequences in [24][25]. Inspired by the ZCZ concept, we apply optimized punctured sequence-pair [26] to ZCZ to construct the new ternary codes– optimized punctured ZCZ sequence-pair set. We also analyze and show that the proposed ternary codes, which have good autocorrelation and cross correlation properties in ZCZ, are good candidates for phase coded waveforms in a RSN.

3.1 The Definition of Optimized Punctured ZCZ Sequence-Pair Set

In this section, we define the ZCZ sequence-pair set and the optimized punctured ZCZ sequence-pair set, and introduce some other useful definitions as the preliminary knowledge.

Definition 3-1: Assume $(\mathbf{X}, \mathbf{Y})$ is a sequence-pair set that consists of $(x_i^{(m)}, y_i^{(m)})$, $m = 0, 1, 2, ..., M-1, i = 0, 1, 2, ..., K-1$, where K is the number of sequence-pairs and M is the length of the sequence-pair. If the following equation is satisfied:

$$R_{x_i y_j}(\tau) = \sum_{m=0}^{M-1} x_i^{(m)} y_j^{*(m+r)} \mod M = \begin{cases} \lambda M, & \text{for } \tau = 0 \text{ and } i = j \\ 0, & \text{for } \tau = 0 \text{ and } i \neq j \\ 0, & \text{for } 0 < |\tau| \leq Z_0 t_b \end{cases} \tag{10}$$

where t_b is the duration of each bit, $\tau = r t_b$ and $0 < \lambda \leq 1$, then $(\mathbf{X}, \mathbf{Y})$ is called ZCZ sequence-pair set. $0 < |\tau| \leq Z_0 t_b$ is the Zero Correlation Zone during which the autocorrelation and cross correlation values could be kept zero. $ZCZPS(M, K, Z_0)$ is an abbreviation.

Definition 3-2 [26] Sequence $\mathbf{u} = (u^{(0)}, u^{(1)}, ..., u^{(M-1)})$ is the punctured sequence for $\mathbf{v} =$

$(v^{(0)}, v^{(1)}, ..., v^{(M-1)})$,

$$u^{(m)} = \begin{cases} 0, & \text{if } m \in p \text{ punctured bits} \\ v^{(m)}, & \text{if } m \in \text{Non-punctured bits} \end{cases} \tag{11}$$

Where p is the number of punctured bits in sequence $\mathbf{v}$, suppose $v^{(m)}\epsilon(-1,1)$ and $u^{(m)}\epsilon(-1,0,1)$, $\mathbf{u}$ is p-punctured binary sequence, $(\mathbf{u},\mathbf{v})$ is called a punctured binary sequence-pair.

Definition 3-3 [26]: The autocorrelation of punctured sequence-pair $(\mathbf{u},\mathbf{v})$ is defined

$$R_{uv}(\tau) = R_{uv}(rt_b) = \sum_{m=0}^{M-1} u^{(m)} v^{*(m+r) \mod M}, 0 \le \tau \le (M-1)t_b \tag{12}$$

If the punctured sequence-pair has the following autocorrelation property:

$$R_{uv}(\tau) = \begin{cases} E, & \text{if } r \equiv 0 \bmod M \\ 0, & \text{others} \end{cases} \tag{13}$$

the punctured sequence-pair is called optimized punctured sequence-pair [26]. Where, $E = \sum_{m=0}^{M-1} u^{(m)} v^{*(m+r) \mod M} = M - p$, is the energy of the punctured sequence-pair.

The punctured sequence-pairs' properties, Fourier transform characteristics, existing necessary conditions and some construction methods with help of already known sequences have been studied by Jiang [26]. An amount of optimized punctured sequence-pairs have been found of length from 3 to 31 so far.

Definition 3-4: If $(\mathbf{X},\mathbf{Y})$ in Definition 3-1 is constructed by optimized punctured sequence-pair and a certain matrix, such as Hadamard matrix or an orthogonal matrix,

$$x_i^{(m)} \in (-1,1), \quad i = 0,1,2,...,M-1$$

$$y_i^{(m)} \in (-1,0,1), \quad i = 0,1,2,...,M-1$$

$$R_{x_i y_j}(\tau) = \sum_{m=0}^{M-1} x_i^{(m)} y_j^{*(m+r) \mod M} = \begin{cases} \lambda M, & \text{for } \tau = 0 \text{ and } i = j \\ 0, & \text{for } \tau = 0 \text{ and } i \ne j \\ 0, & \text{for } 0 < |\tau| \le Z_0 t_b \end{cases} \tag{14}$$

where $\tau = rt_b$ and $0 < \lambda \leq 1$, then $(\mathbf{X}, \mathbf{Y})$ can be called an optimized punctured ZCZ sequence-pair set, and we use $OPZCZPS(M, K, Z_0)$ as its abbreviation.

Definition 3-5: The autocorrelation function (ACF) (here we use autocorrelation to distinguish the cross correlation between two different sequences of a sequence-pair from the cross correlation between two different sequence-pairs) of sequence-pair $(\mathbf{x}_i, \mathbf{y}_i)$ is defined by:

$$R_{x_i y_i}(\tau) = \sum_{m=0}^{M-1} x_i^{(m)} y_i^{*(m+r) \mod M} \tag{15}$$

The cross correlation function (CCF) of two sequence-pairs $(\mathbf{x}_i, \mathbf{y}_i)$ and $(\mathbf{x}_j, \mathbf{y}_j), i \neq j$ is defined by:

$$R_{x_i y_j}(\tau) = \sum_{m=0}^{M-1} x_i^{(m)} y_j^{*(m+r) \mod M} \tag{16}$$

Where $\tau = rt_b$ is the time delay and t_b is the bit duration.

3.2 Design for an Optimized Punctured ZCZ Sequence-pair Set

Based on an odd length optimized punctured binary sequence-pair and a Hadamard matrix, we provide a method to construct an optimized punctured ZCZ sequence-pair set.

Step 1: Choosing an odd length optimized punctured binary sequence-pair $(\mathbf{u}, \mathbf{v})$, the length of each sequence is M_1

$$\mathbf{u} = u^{(0)}, u^{(1)}, ..., u^{(M_1-1)}, u^{(m)} \in (-1, 1),$$

$$\mathbf{v} = v^{(0)}, v^{(1)}, ..., v^{(M_1-1)}, v^{(m)} \in (-1, 0, 1),$$

$$n = 0, 1, 2, ..., M_1 - 1$$

Step 2: Considering a Hadamard matrix $\mathbf{B}$ of order M_2, the length of each sequence in $\mathbf{B}$

equals to the number of the sequences as M_2. Here, $\mathbf{b}_i$ is the row vector.

$$\mathbf{B} = [\mathbf{b}_0; \mathbf{b}_1; ...; \mathbf{b}_{M_2-1})],$$

$$\mathbf{b}_i = (b_i^{(0)}, b_i^{(1)}, ..., b_i^{(M_2-1)}),$$

$$R_{\mathbf{b}_i\mathbf{b}_j} = \begin{cases} M_2, & \text{if } i = j \\ 0, & \text{if } i \neq j \end{cases}$$

Step 3: Doing bit-multiplication on the optimized punctured binary sequence-pair and each row of Hadamard matrix $\mathbf{B}$, then we obtain the sequence-pair set $(\mathbf{X}, \mathbf{Y})$,

$$\mathbf{b}_i = (b_i^{(0)}, b_i^{(1)}, ..., b_i^{(M_2-1)}), i = 0, 1, ..., M_2 - 1,$$

$$x_i^{(m)} = u^{(m \mod M_1)} b_i^{(m \mod M_2)}, 0 \leq i \leq M_2 - 1, 0 \leq m \leq M - 1,$$

$$\mathbf{X} = (\mathbf{x}_0; \mathbf{x}_1; ...; \mathbf{x}_{M_2-1}),$$

$$y_i^{(m)} = v^{(n \mod M_1)} b_i^{(m \mod M_2)}, 0 \leq i \leq M_2 - 1, 0 \leq m \leq M - 1,$$

$$\mathbf{Y} = (\mathbf{y}_0; \mathbf{y}_1; ...; \mathbf{y}_{M_2-1})$$

Since the optimized punctured binary sequence-pairs used here are of odd lengths and the length of Walsh sequence in Hadamard matrix is $2^k, k = 1, 2, ...$, we obtain that $GCD(M_1, M_2) = 1$ (greatest common divisor of M_1 and M_2 is 1) and $M = M_1 * M_2$.

To sum up, the sequence-pair set $(\mathbf{X}, \mathbf{Y})$ is an optimized punctured ZCZPS and $Z_0 = M_1 - 1$ is the Zero Correlation Zone. The length of each sequence in the optimized punctured ZCZ sequence-pair set is $M = M_1 * M_2$ that depends on the product of the length of the optimized punctured sequence-pair and the length of the Walsh sequence in the Hadamard matrix. The number of sequence-pairs in $(\mathbf{X}, \mathbf{Y})$ rests on the order of the Hadamard matrix. The sequence $\mathbf{x}_i$ in the sequence set $\mathbf{X}$ and the corresponding sequence $\mathbf{y}_i$ in the sequence set Y construct an optimized punctured ZCZ sequence-pair $(\mathbf{x}_i, \mathbf{y}_i)$ that can be used as a phase coded waveform pair. The correlation property of the sequence-pairs in the optimized punctured ZCZ sequence-pair set could

be illustrated as:

$$R_{x_i y_j}(\tau) = R_{uv}((r \mod M_1)t_b) R_{b_i b_j}((r \mod M_2)t_b) = \begin{cases} EN_2, & \text{if } r = 0 \text{ and } i = j \\ 0, & \text{if } 0 < |r| \leq M_1 - 1 \text{ and } i = j \\ 0, & \text{if } i \neq j \end{cases} \quad (17)$$

where $\tau = rt_b$ is the time delay and t_b is one bit duration.

It is easy to prove that the constructed sequence-pair set $(\mathbf{X}, \mathbf{Y})$ is an optimized punctured ZCZ sequence-pair set. The proof in detail could be refered to Appendix 1.

3.3 Properties of Optimized Punctured ZCZ Sequence-pair set

We study the autocorrelation and cross correlation properties of an OPZCZPS which is constructed by the above method. For example, the 28-bit long optimized punctured ZCZPS $(\mathbf{X}, \mathbf{Y})$ is constructed by the 7-bit long optimized punctured binary sequence-pair $(\mathbf{u}, \mathbf{v}), \mathbf{u} = [+++-\!-\!-+$ $-+-+++-\!-\!-\!-+-\!-+-\!-+++-++-]$, $\mathbf{v} = [++++000+0+0+++0000+00+00+++0++0]$ (using $'+'$ and $'-'$ symbols for $'1'$ and $'-1'$) and the Hadamard matrix $\mathbf{B}$ of order 4. The number of sequence-pairs in $(\mathbf{X}, \mathbf{Y})$ is 4, and the length of the sequence-pair is $7 * 4 = 28$. The first row of each matrix $\mathbf{X} = [\mathbf{x}_1; \mathbf{x}_2; \mathbf{x}_3; \mathbf{x}_4]$ and $\mathbf{Y} = [\mathbf{y}_1; \mathbf{y}_2; \mathbf{y}_3; \mathbf{y}_4]$ constitute a certain optimized punctured ZCZP $(\mathbf{x}_1, \mathbf{y}_1)$. Similarly, the second row of each matrix $\mathbf{X}$ and $\mathbf{Y}$ constitute another optimized punctured ZCZ sequence-pair $(\mathbf{x}_2, \mathbf{y}_2)$ and so on.

$$\begin{aligned} \mathbf{x}_1 &= [+++--+-+++--+-+++--+-+++--+-], \\ \mathbf{y}_1 &= [+++00+0+++00+0+++00+0+++00+0]; \\ \mathbf{x}_2 &= [+-++----+--++++-++-----+--++], \\ \mathbf{y}_2 &= [+-+00-0-+-00+0+-+00-0-+-00+0]. \\ &\ldots \end{aligned}$$

3.3.1 Autocorrelation and Cross Correlation Properties of the Optimized Punctured ZCZ Sequence-pair Set

The autocorrelation and the cross correlation property of the optimized punctured ZCZ sequence-pair set $(\mathbf{X}, \mathbf{Y})$ constructed by the 28-bit long optimized punctured ZCZ sequence-pairs are illustrated in Figs. 1 and 2.

According to Figs. 1 and 2, the autocorrelation function (ACF) sidelobe of one optimized punctured ZCZ sequence-pair and the cross correlation function (CCF) of two different optimized punctured ZCZ sequence-pairs can be kept as low as 0 when the time delay is kept within $Z_0 = M_1 - 1 = 6$ (Zero Correlation Zone).

It is known that a traditional criterion for evaluating code of length M is the signal peak to sidelobe ratio (PSR) of their aperiodic ACF, which can be bounded by [27]

$$[PSR]_{dB} \leq 20logM = [PSR_{max}]_{dB} \tag{18}$$

The only uniform aperiodic phase codes that can reach the PSR_{max} are the Barker codes [28] whose length is equal or less than 13. Considering the periodic sequences, the m-sequences or Legendre sequences could achieve the lowest periodic ACF of $|R_i(\tau \neq 0) = 1|$ for the binary sequences. For non-binary sequences, it is possible to find perfect sequences of ideal ACF. Golomb codes are a kind of two-valued (biphase) perfect codes which obtain zero periodic ACF but result in large mismatch power loss. The Ipatov code shows a way of designing code pairs with perfect periodic autocorrelation (the cross correlation of the code pair) and minimal mismatch loss, but has a complicated reference code and construction method. Zero periodic ACF for all nonzero shifts could be obtained by polyphase codes, such as Frank and Zadoff codes, but the more complicated constructing methods and implementation cost are required. In general, for both binary and non-binary sequences in the periodic sequence field, it is not possible for the sequences to have

perfect CCF and ACF simultaneously although ideal CCFs could be achieved alone. Nevertheless, according to Figs. 1 and 2, it is obvious that ACF and CCF sidelobes of the new code could reach as low as zero. Stating differently, the PSR can be as large as infinite. The reference sequence of our proposed codes is ternary $[-1, 0, 1]$ which is less complicated than some other perfect codes such as Ipatvo code. The reference code for Ipatov code is of a three-element alphabet which might not always be integer.

Nevertheless, there might be the concern that multiple peaks of ACF in Fig. 1 might introduce ambiguity to range resolution. We are studying the single target system in this paper and assume that the PRF (pulse repetition frequency) is well controlled. The only concern is that multiple peaks of one transmit signal reflected by one target may affect determining the main peak of ACF. However, these multiple peaks could have an advantage for the matched filter. Based on the multiple peaks, the matched filter could shift at the period of ZCZ length to track each peak instead of shifting bit by bit after the first peak is acquired. Hence, the matched filter could work more efficiently in this way. Alike the tracking technology in synchronization of CDMA system, checking several peaks instead of only one peak guarantee the precision of P_D and avoidance of P_{FA}.

3.3.2 Ambiguity Function of One Optimized Punctured ZCZ Sequence-pair

When the transmitted impulse is reflected by a moving target, the reflected echo includes a linear phase shift which corresponds to a Doppler shift F_D [6]. As a result of the Doppler shift F_D, the main peak of the autocorrelation function is reduced and so as to the SNR degradation shown as following:

$$[d]_{dB} = 10log\frac{\int_{-T/2}^{T/2} x(t)x^*(t)dt}{\int_{-T/2}^{T/2} x(t)e^{j2\pi F_D t}x^*(t)dt} \tag{19}$$

The sidelobe structure is also changed because of the Doppler shift.

Considering the sequence-pair $(\mathbf{x}, \mathbf{y})$ and the periodic correlation property of the sequence-pair, we use the single-periodic ambiguity function [21] and rewrite it as

$$A(\tau, F_D) = |\frac{1}{T}\int_{-T/2}^{T/2} x(t)exp(j2\pi F_D t)y^*(t-\tau)dt| \tag{20}$$

Equation (20) can be used to analyze the autocorrelation performance within Doppler shift, and is plotted in Fig. 3(a) in a three-dimensional surface plot to analyze the time-Doppler performance of the OPZCZP. In addtion, the ambiguity function of the Ipatov code of length 24 is also illustrated in Fig. 3(b). Here, maximal time delay is 1 unit (normalized to length of the code, in units of Mt_b) and maximal Doppler shift is 3 units for ACF (normalized to the inverse of the length of the code, in units of $1/(Mt_b)$). From Fig. 3(a), it is easy to see that there is relative uniform plateau suggesting low and uninform sidelobes, minimizing target masking effect in zero correlation zone of time domain, where $Z_0 = 6$, $-6t_b < \tau < 6t_b, \tau \neq 0$. Obeserving Fig. 3(b), zero sidelobe could be obtained when there is no Doppler shift, however, when Doppler shift increases there is obvious convex surface comparing with Fig. 3(a). Hence, our codes are better tolerant of large Doppler shift than the Ipatov codes. Stating differently,

when Dopper shift is introduced to the system, our codes perform better than Ipatov codes.

3.3.3 Ambiguity Function under the Interference from Other Radar Sensors

Considering interference from another radar sensor j, the ambiguity function of ith radar sensor can be expressed as

$$A_i(\tau, F_{D_i}, F_{D_j}) = |\frac{1}{T}\int_{-T/2}^{T/2} (x_i(t)exp(j2\pi F_{D_i}t) + x_j(t)exp(j2\pi F_{D_j}t))y_i^*(t-\tau)dt| \tag{21}$$

Where τ is the time delay between the ith transmit radar sensor and its corresponding matched filter, F_{D_i} and F_{D_j} are the Doppler shift for signals transmitting from ith and jth radar sensors

respectively.

Fig. 4(a) is a three-dimensional surface plot to analyze the ambiguity function of ith radar sensor (considering interference from jth radar sensor). Since there are not mature phase coded waveforms for RSN available, we provide the time-Doppler performance of the widely used spread spectrums codes-Gold codes in Fig. 4(b) to compare with our codes. Comparing Fig. 4(a) with Fig. 3(a), it is easy to see that there is relative uniform plateau suggesting low and uninform sidelobes, minimizing target masking effect in zero correlation zone of time domain, where $Z_0 = 6$, $-6t_b < \tau < 6t_b, \tau \neq 0$ when Doppler shift is not large. As a result, the interference from another radar j increases the our codes' unintolerance of large Doppler shift. Observing Fig. 4(b), there is neither uniform nor low plateau among the whole figure. There are still some high peak sidelobes due to the unideal AFC of the Gold codes even if the Doppler shift is zero.

The output of matched filter of ith radar sensor (considering interference from jth radar sensor) is illustrated in Fig. 5 under the condition of no Doppler shift. According to Fig. 5(a), there are regular high peaks on multiples of period 7 that is the length of the optimized punctured sequence-pair used in the constructing method. And the sidelobe can be as low as zero when the time delay is kept among zero correlation zone $-6t_b \leq \tau \leq 6t_b, \tau \neq 0$. The high peak on zero time delay point can be used to detect targets. However, the Fig. 5(b) shows that the sidelobes of ACF of the Gold codes are seriously interfered which could have bad effect on the range resolution.

4 System Simulation of Radar Sensor Network

4.1 Detection of RSN

Assume that there are N transmit radar sensors in a RSN, the combined signal for ith receiving radar is

$$r_i(u,t) = \sum_{j=1}^{N} x_j(t-t_j)exp(j2\pi F_{D_j}t) + n(u,t) \tag{22}$$

where $x_j(t)$ is the transmitting signal and F_{D_j} is the Doppler shift of the reflected signal of jth transmit radar sensor. t_j is the time delay between the signals reflected by jth transmit radar sensor and ith transmit radar sensor. When $j = i$, the time delay between two reflected signals is zero $t_i = 0$. $n(u,t)$ is the additive white Gaussian noise (AWGN).

According to the structure illustrated in Fig. 6, the received signal $r_i(u,t)$ is processed by the corresponding matched filter $y_i(t)$ and the output of branch i is $Z_i(u,\tau)$. Then the output of branch i is

$$|Z_i(u,\tau)| = |\int_{-T/2}^{T/2}[\sum_{j=1}^{N} x_j(t-t_j)exp(j2\pi F_{D_j}t) + n(u,t)]y_i^*(t-\tau)dt| \tag{23}$$

where τ is the time delay between the matched filter $y_i(t)$ and ith transmit radar sensor. Assume that we could obtain high-resolution measurements of targets in range ($\tau = 0$), the ideal output is $|Z_i(u,0)| = |\int_{-T/2}^{T/2}[\sum_{j=1}^{N} x_j(t-t_j)exp(j2\pi F_{D_j}t) + n(u,t)]y_i^*(t)dt|$ and $n(u) = \int_{-T/2}^{T/2} n(u,t)y_i^*(t)dt$ can be easily proved to be an AWGN.

We investigate $|Z_i(u,0)|$ in three special cases:

1) If all the radar sensors of RSN transmit signals synchronously and the target is not moving, stating differently, there is neither time delay for each transmit radar sensor nor Doppler shift, $t_1 = t_2 = ... = t_N = 0$ and $F_{D_1} = F_{D_2} = ... = F_{D_N} = 0$, then

$$|Z_i(u,0)| = |\int_{-T/2}^{T/2}[\sum_{j=1}^{N} x_j(t) + n(u,t)]y_i^*(t)dt| = |E + 0 + n(u)| \tag{24}$$

where $E = \int_{-T/2}^{T/2} x_i(t) y_i^*(t) dt$.

2) Considering Doppler shift and all the radar sensors of RSN still transmit signals synchronously, $t_1 = t_2 = ... = t_N = 0$, then

$$|Z_i(u,0)| = |\int_{-T/2}^{T/2} [\sum_{j=1}^{N} x_j(t) exp(j2\pi F_{D_j}) + n(u,t)] y_i^*(t) dt| \tag{25}$$

A Doppler shift compensation factor $exp^*(j2\pi F_{D_i})$ is applied to the ith receive radar sensor and F_{D_i} is the estimated Doppler shift corresponding to the ith receive radar sensor. The equation (25) can be modified as

$$\begin{aligned} |Z_i(u,0)| &= |\int_{-T/2}^{T/2} [\sum_{j=1}^{N} x_j(t) exp(j2\pi F_{D_j}) + n(u,t)] y_i^*(t) exp^*(j2\pi F_{D_i} t) dt| \\ &\leq |E| + |\int_{-T/2}^{T/2} [\sum_{j\neq i}^{N} x_j(t) exp(j2\pi (F_{D_j} - F_{D_i})) y_i^*(t)| + |\int_{-T/2}^{T/2} n(u,t) y_i^*(t) exp^*(j2\pi F_{D_i} t) dt| \end{aligned} \tag{26}$$

If the Doppler shift could be precisely estimated on the receive radar sensor, it is reasonable to have $F_{D_1} = F_{D_2} = ... = F_{D_j} = F_D$ here. The equation (26) can be further simplified as

$$|Z_i(u,0)| \leq |E| + 0 + |\int_{-T/2}^{T/2} n(u,t) y_i^*(t) exp^*(j2\pi F_{D_i} t) dt| \tag{27}$$

3) Considering Doppler shift and all the radar sensors of RSN transmitting signals asynchronously, the Doppler shift compensation factor is applied to the receive radar sensor as well,

$$\begin{aligned} & |Z_i(u,0)| \\ = \; & |\int_{-T/2}^{T/2} [\sum_{j=1}^{N} x_j(t-t_j) exp(j2\pi F_{D_j} t) + n(u,t)] y_i^*(t) exp^*(j2\pi F_{D_i} t) dt| \\ \leq \; & |\int_{-T/2}^{T/2} [\sum_{j=1}^{N} x_j(t-t_j) exp(j2\pi (F_{D_j} - F_{D_i}))] y_i^*(t)| + |\int_{-T/2}^{T/2} n(u,t) y_i^*(t) exp^*(j2\pi F_{D_i} t) dt| \end{aligned} \tag{28}$$

Similarly, we assume that $F_{D_1} = F_{D_2} = ... = F_D$, then

$$|Z_i(u,0)| \leq |E| + |\int_{-T/2}^{T/2} [\sum_{j\neq i}^{N} x_j(t-t_j)] y_i^*(t) dt| + |\int_{-T/2}^{T/2} n(u,t) y_i^*(t) exp^*(j2\pi F_{D_i} t) dt| \tag{29}$$

Since our codes hold ideal periodic ACF and CCF in ZCZ, we modify the frame of received data before the matched filter. The frame of received data is illustrated in Fig. 7. The data from bit $M+1$ to bit $\max(t_j)+M$ are added to the data from bit 1 to bit M, bit by bit. It is easy to observe that $|\int_{-T/2}^{T/2}[\sum_{j\neq i}^{N} x_j(t-t_j)]y_i^*(t)dt| = 0$. Therefore, equation (29) turns to be

$$|Z_i(u,0)| \leq |E| + 0 + |\int_{-T/2}^{T/2} n(u,t)y_i^*(t)exp^*(j2\pi F_{D_i}t)dt| \tag{30}$$

Observing the equations (27) and (30), it is easy to see that $|Z_i(u,0)|$ in case 2) and case 3) can be theoretically comparable if the frame is modified before the matched filter in case 3). Stating differently, the RSN using our codes provide promising performance even if all the radar sensors transmit signal asynchronously.

Observing equations (24), (27) and (30), $n(u)$ is AWGN and $\int_{-T/2}^{T/2} n(u,t)y_i^*(t)exp^*(j2\pi F_{D_i}t)dt$ can be easily proved to be AWGN as well. Let $w_i = |Z_i(u,0)|$, if there is a target, then w_i follows Rician distribution and the probability density function (pdf) of y_i is

$$f_s(w_i) = \frac{2w_i}{\sigma^2}exp[-\frac{(w_i^2+\lambda^2)}{\sigma^2}]I_0(\frac{2\lambda w_i}{\sigma^2}) \tag{31}$$

where $\lambda = E = \int_{-T/2}^{T/2} x_i(t)y_i^*(t)dt$, σ^2 is the noise power and $I_0(\cdot)$ is the zero-order modified Bessel function of the first kind. If there is no target, then w_i follows Rayleigh distribution and the probability density function (pdf) of w_i is

$$f_n(w_i) = \frac{w_i}{\sigma^2}exp[-\frac{(w_i^2)}{\sigma^2}] \tag{32}$$

where σ^2 is the noise power.

Similar to the diversity combining to combat channel fading in communications, we use the equal gain combining method to combine all the $|Z_i(u,0)|$. Assume all the radar sensors are working independently and $\mathbf{w} = [w_1, w_2, ..., w_N]$, then the pdf of $\mathbf{w}_s$ for targets existence is

$$f(\mathbf{w}_s) = \sum_{i=1}^{N} f_s(w_i) \tag{33}$$

and

$$f(\mathbf{w}_n) = \sum_{i=1}^{N} f_s(w_i) \tag{34}$$

for $\mathbf{w}_n$ when there is no target. Finally, we apply Bayesian's rule to obtain the decision criterion, which is

$$\frac{f(\mathbf{w}_s)}{f(\mathbf{w}_n)} \underset{Notarget}{\overset{Targetexists}{\gtrless}} \frac{P_n}{P_s} \tag{35}$$

where P_n represents the probability of no targets but noise and P_s denotes the probability fo target occurrence.

4.2 System Simulation

4.2.1 Simulation Environment

We simulated the performance versus different number of radars in RSN under the condition with Doppler shift or without Doppler shift. According to [29], P_D (Probability of Detection), P_{FA} (Probability of False Alarm) and P_M (Probability of Miss) are common parameters of most interest in the radar system. Note that $P_M = 1 - P_D$, thus, P_D and P_{FA} suffice to specify the probabilities of interest in radar system. Hence, we respectively simulated P_D and P_{FA} of RSN consisting of different number of radar sensors. We simulated P_D and P_{FA} of a single radar system using the optimized punctured ZCZ sequence-pairs, and compared its performance with the single radar system using the Barker code and the Ipatov code respectively. We also simulate P_D and P_{FA} of 4-radar and 8-radar RSNs which use the optimized punctured ZCZ sequence-pairs as the pulse compression codes and compared their performances with the 4-radar and 8-radar RSNs using the Gold codes. In addition, we simulate P_D and P_{FA} under the three different conditions which are the multiple radar sensors transmit signal synchronously and the target is immovable, the multiple radar sensors transmit signal synchronously and the target is moving and the multiple radar sensors

transmit signal non-synchronously and the target is moving. 10^5 times of Monte-Carlo simulation has been run for each SNR value. When multiple radar sensors work in RSN to detect a single moving target, we assume that the Doppler shift can be precisely estimated and the compensating factors of the Doppler shift are used in the receiving radar sensors.

4.2.2 Results and Analysis

The P_D and P_{FA} of single radar, 4-radar, 8-radar systems are compared respectively in Fig. 8 under the first condition that multiple radar sensors transmit signal synchronously and the target is immovable. According to Fig. 8(a), to achieve the same $P_D = 10^{-0.01}$, the single radar system using our codes requires about 0.15dB of SNR greater than the single radar system using the Barker code, but requires 0.2dB of SNR less than the single radar system using the Ipatov code. In addition, the 4-radar system using our codes could save 1.1dB of SNR than the single radar system using the Ipatov code and save 0.3dB of SNR than the 4-radar system using the Gold codes when $P_D = 10^{-0.01}$. As the number of radar sensors increases to 8, P_D of the 8-radar system using our codes is further increased and much larger than P_D of the 8-radar system using the Gold codes. Fig. 8(b) shows that to obtain the same $P_{FA} = 10^{-2}$, the SNR of a single radar system using our code is 0.3dB less than that of a single radar system uing the Barker code and 0.4dB less than that of a single radar using the Ipatov code. Increasing the number of radar sensors in RSN, when $P_{FA} = 10^{-2}$, the 8-radar system using our codes requires about 2dB of SNR less than the single radar system using the Ipatov code, about 0.7dB of SNR less than the 4-radar system using our codes and 0.5dB of SNR less than the 8-radar system using the Gold codes. It is easy to see that the single radar system using our proposed codes works better than the single radar system using the Barker codes, but worse than the single radar system using the Ipatov codes, which matches up to the properties of these codes. However, the Ipatov codes have a reference code with a three-element

alphabet which is more complicated and costs much more energy for implementation comparing with our codes. Both P_D and P_{FA} could be improved by applying more radar sensors to a RSN. As a result, RSN using our codes could provide promising detection performance which is much better than that of RSN using the same number of Gold codes.

The P_D and P_{FA} of single radar, 4-radar, 8-radar systems are illustrated respectively in Fig. 9 under the second condition that multiple radar sensors transmit signal synchronously and the target is moving. Observing Fig. 9(a), when $P_D = 10^{-0.01}$, the SNR of a single radar system using our code is about 0.15dB less than that of a single radar system using the Barker code and about 0.1dB more than that of a single radar using the Ipatov code. The 4-radar system using our codes could save 1.2dB of SNR than the single radar system using the Ipatov code and save 0.4dB of SNR than the 4-radar system using the Gold codes. Applying our codes to the 8-radar system, P_D is increased and is much larger than the 8-radar system using the Gold codes. According to Fig. 9(b), to achieve the same $P_{FA} = 10^{-2}$, the single radar system using our codes requires about 0.3dB of SNR more than the single radar system using the Barker code, but requires 0.4dB of SNR less than the single radar system using the Ipatov code. Meanwhile, the 8-radar system using our codes could gain about 2.2dB of SNR more than the single radar system using the Ipatov code, about 0.9dB of SNR more than that of 4-radar system using our codes and 0.5dB of SNR more than the 8-radar system using the Gold codes when $P_{FA} = 10^{-2}$. In this case, the target is moving, so the Doppler shift is considered here. It is easy to draw the similar conclusion that the single radar system using our proposed codes could work better than the single radar system using the Barker codes, but worse than the single radar system using the Ipatov codes. More radar sensors could be applied to improve P_D and P_{FA}, and our codes could perform better than the Gold codes in a RSN consisting of the same number of radar sensors.

If multiple radar sensors transmit signal asynchronously, stating differently, there are time delay

among all the transmit radar sensors, we consider the RSN consisting of no less than two radar sensors. Hence, we simulate P_D and P_{FA} of 4-radar and 8-radar systems in Fig. 10(a) and Fig. 10(b) under the third condition that the multiple radar sensors transmit signal asynchronously and the target is moving. Observing Fig. 10(a), to obtain the same $P_D = 10^{-0.01}$, the 4-radar system using our codes requires about 0.7dB of SNR more than the 4-radar system using the Gold codes. The Fig. 10(b) illustrates that the SNR of 8-radar system using our codes is about 0.5dB less than that of 8-radar system using the Gold codes and about 1dB more than that of a 4-radar system using our codes, when $P_{FA} = 10^{-2}$. Both P_D and P_{FA} could be improved by increasing the number of radar sensors in a RSN. In this case, the advantage of our codes is more obvious over the Gold codes, because our codes have the better cross correlation property and the modified frame is used. The RSN using our codes could perform much better than the RSN using the same number of Gold codes even if the Doppler shift and time delay among transmit radar sensors are both considered.

Comparing Fig. 8 and Fig. 9, it is clear to see that, no matter how many radar sensors have been exploited in the RSN, the performances of system considering Doppler shift are worse than but close to the performance of system working under the condition of no Doppler shift. Since the Doppler shift is assumed to be precisely estimated and well compensated in the receive radar sensor, the performances under the above two different conditions are so close. However, we could still discover that the performance reduction of the single radar system is more serious than that of the RSN consisting of multiple radar sensors when Doppler shift is considered. Therefore, our codes could be applied to a RSN consisting of multiple radar sensors to cope with the unfavorable effect of the Doppler shift. It is also clearly see that no matter whether the target is moving or not, performance of detection of RSN employing our optimized punctured ZCZPS and equal gain combination are superior to that of the RSN using Gold codes, and are much better than the single radar system. In conclusion, the more radar sensors the RSN consists of, the better

performance it provides. When multiple radar sensors transmit signal asynchronously, P_D and P_{FA} of RSN using our codes could still be comparable to those under the condition that multiple radar sensors transmit signal synchronously. As a result, the optimized punctured ZCZPS could perform promisingly in RSN under all the three different conditions.

5 Conclusions

In this paper, we have studied the phase coded waveforms design for the radar sensor networks (RSN). We provide a new ternary codes–the optimized punctured ZCZPS which could be used as the phase coded waveforms in a RSN. The significant advantage of the optimized punctured ZCZPS is the considerably reduced sidelobe as low as zero and zero mutual cross correlation value in the zero correlation zone (ZCZ). Based on the ideal orthogonal property of the proposed codes, they can coexist in the RSN and achieve better detection performance than that of a RSN using other orthogonal codes such as the Gold codes. Consequently, the optimized punctured ZCZPS could be effectively applied to RSN in order to satisfy higher demands criterion for detection accuracy of the RSN in the modern military and security affairs.

Appendix 1

Proof:

1) When $i = j$,

$$r = 0,$$

$$R_{uv}(0) = E, R_{b_i b_j}(0) = M_2, R_{x_i y_j}(0) = R_{uv}(0) R_{b_i b_j}(0) = EM_2;$$

$$0 < |r| \leq M_1 - 1,$$

$$R_{uv}(rt_b) = 0, R_{x_i y_j}(rt_b) = R_{uv}((r \mod M_1)t_b) R_{b_i b_j}((r \mod M_2)t_b) = 0;$$

2) When $i \neq j$,

$$r = 0,$$

$$R_{b_i b_j}(0) = 0, R_{x_i y_j}(0) = R_{x_j y_i}(0) = R_{uv}((r \mod M_1)t_b) R_{b_i b_j}((r \mod M_2)t_b) = 0;$$

$$0 < |r| \leq M_1 - 1,$$

$$R_{uv}(rt_b) = 0, R_{x_i y_j}(rt_b) = R_{uv}((r \mod M_1)t_b) R_{b_i b_j}((r \mod M_2)t_b) = 0.$$

According to **Definition 3-1** and **Definition 3-4**, $(\mathbf{X}, \mathbf{Y})$ constructed by the above method is an optimized punctured ZCZ sequence-pair set.

Acknowledgement

This work was supported in part by the National Science Foundation under Grants CNS-0964713, CCF-0956438, CNS-1050618, CNS-0831902, CNS-0721515, and Office of Naval Research (ONR) under Grant N00014-07-1-0395 and N00014-07-1-1024.

References

[1] M. R. Bell, "Information theory and radar waveform design," *IEEE Trans on Information Theory,* vol. 39, no. 5, pp. 1578-1597, Sept. 1993.

[2] S. Sowelam and A. Tewfik, "Waveform selection in radar target classification," *IEEE Trans on Information Theory,* vol. 46, no. 3, pp. 1014-1029, 2000.

[3] Q. Liang, "Waveform Design and Diversity in Radar Sensor Networks: Theoretical Analysis and Application to Automatic Target Recognition," *IEEE Sensor and Ad Hoc Communications and Networks Conference,* vol. 2, no. 28, pp. 684-689, Sep. 2006.

[4] Q. Liang, "Collaborative Signal Processing Using Radar Sensor Networks," *IEEE Military Communications Conference,* 23-25, pp. 1-6, Oct. 2006.

[5] Q. Liang, "Radar Sensor Networks for Automatic Target Recognition with Delay-Doppler Uncertainty," *IEEE Military Communications Conference,* 23-25, pp. 1-7, Oct. 2006.

[6] M. A. Richards, *Fundamentals of Radar Signal Processing,* McGraw-Hill, 2005.

[7] S. W. Golomb, "Two-valued sequences with perfect autocorrelation", *IEEE Transactions on Aerospace and Electronic Systems,* AES-28(2), pp. 382-386, March 1992.

[8] V. P. Ipatov, *Periodic Discrete Signals with Optimal Correlation Properties,* Radio I Svyaz, Moscow, 1992.

[9] R. Sato and M. Shinrhu, "Simple mismatched filter for binary pulse compression code with small PSL and small S/N loss [radar]", *IEEE Transactions on Aerospace and Electronic Systems,* AES-39(2), pp. 711-718, April 2003.

[10] K. Sato, H. Horie, H. Hanado and H. Kumagai, "A digital-analog hybrid technique for low range sidelobe pulse compression", *IEEE Transactions on Aerospace and Electronic Systems,* AES-39(7), pp. 1612-1615, July 2001.

[11] A. Tanner, S. L. Durden, R. Denning, E. Im, F. K. Li, W. Ricketts and W. Wilson, "Pulse compression with very low sidelobes in an airborne rain mapping radar", *IEEE Transactions on Aerospace and Electronic Systems,* AES-32(1), pp. 211-213, Jan. 2004.

[12] L. R. Welch, "Lower bounds on the maximum cross correlation of signals," *IEEE Trans. Inform. Theory*, IT-20, (3), pp. 397-399, 1974.

[13] V. M. Sidelnikov, "On mutual correlation of sequences," *Soviet Math doklady*, 12,pp. 197-201, 1971.

[14] D. V. Sarwate and M .B. Pursley, "Crosscorrelation properties of pseudorandom and related sequences," *Proc. IEEE*, 68, (3), pp. 593-620, 1980.

[15] P. G. Boyvalenkov, D. P. Danev and S.P. Bumova, "Upper bounds on the minimum distance of spherical codes," *IEEE Trans. Inform. Theory*, 42, (5), pp. 1576-1581, 2002.

[16] P. Z. Fan and M. Darnell, *Sequence design for communications applications,* Research Studies Press, John Wiley & Sons Ltd, London, 1996.

[17] P. Z. Fan and M. Darnell, "On the construction and comparison of period digital sequences sets," *IEE Proc. Commun.*, 144, (6), pp. 111-117, 1997.

[18] P. Z. Fan, N. Suehiro, N. Kuroyanagi and X. M. Deng, "A class of binary sequences with zero correlation zone," *IEE Electron.Letter*, 35 (10): 777-779, 1999.

[19] P. Woodward, *Probability and Information Theory, with applications to Radar.* New York: Pergamon, 1957.

[20] P. Woodward, Radar ambiguity analysis Tech. Rep. RRE Technical Note No. 731, Feb. 1967

[21] H. Levanon and A. Freedman, "Periodic ambiguity function of CW signals with perfect periodic autocorrelation," *IEEE Trans on Aerospace and Electronic systems,* vol. 28, no. 2, pp. 387-395, Apr. 1992.

[22] P. Z. Fan and L. Hao, "Generalized Orthogonal Sequences and Their Applications in Synchronous CDMA Systems," *IEICE Trans.Fundamentals*, E832A(11): 1 16, 2000.

[23] P. Z. Fan, "New Direction in Spreading Sequence Design and the Related Theoretical Bounds," *International Conference of Communications , Circuits and Systems*, Jun. 29-Jul. 1, 2002, PRC.

[24] S. Matsufuji, N Suehiro , N Kuroyanagi and P Z Fan, "Two types of polyphase sequence set for approximately synchronized CDMA systems," *IEICE Trans. Fundamentals*, E862A(1): 229-234, Jan. 2003.

[25] H. Torii, M. Nakamura and N. Suehiro, "A new class of zero correlation zone sequences," *IEEE Tran. Inform.Theory*, 50: 559-565, Mar. 2004.

[26] T. Jiang, *Research on Quasi-Perfect Binary Signal Pair and Perfect Punctured Binary Signal Pair Theory,* Ph.D Dissertation: Yanshan University, 2003.

[27] M. I. Skolnik, *Radar Handbook,* New York: McGraw-Hill, 1970.

[28] R. H. Barker, "Group Synchronizing of Binary Digital Sequences," *Communication Theory,* pp. 273-287, 1953.

[29] S. Ariyavisitakul, N. Sollenberger, and L. Greenstein, *Introduction to Radar System,* Tata McGraw-Hill, 2001.

List of Figures

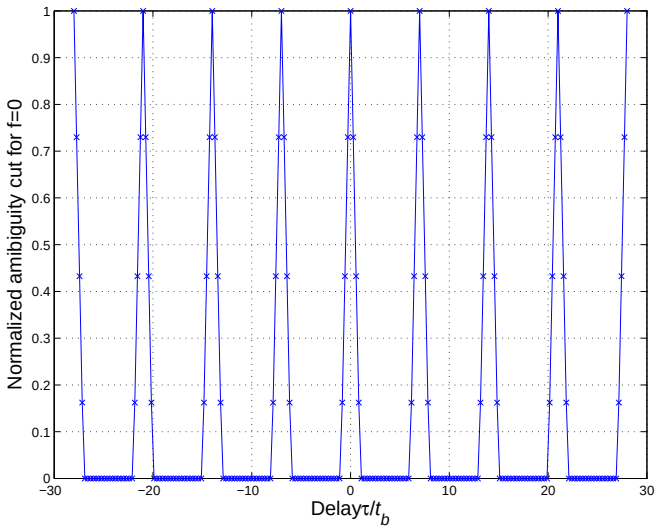

Figure 1: Periodic autocorrelation property of optimized punctured ZCZPS

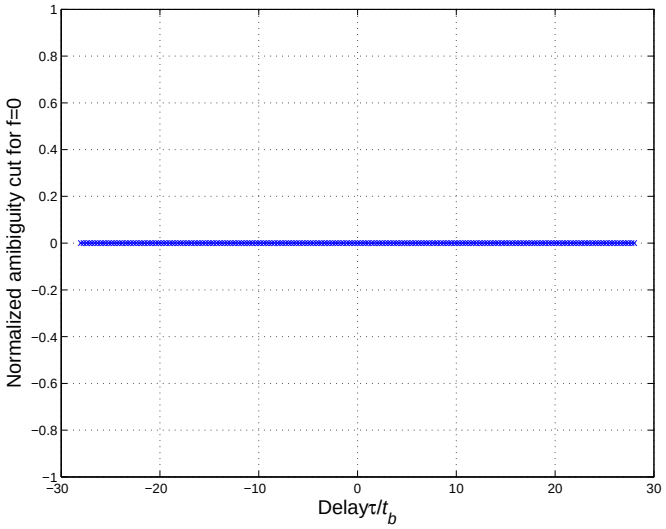

Figure 2: Periodic cross correlation property of optimized punctured ZCZPS

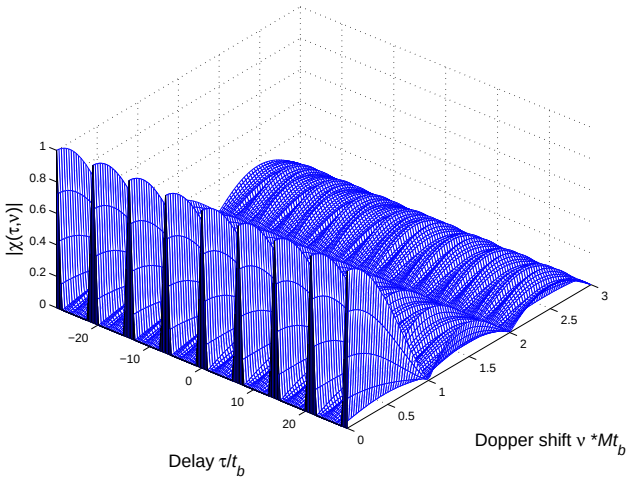

(a)28-length ZCZPS

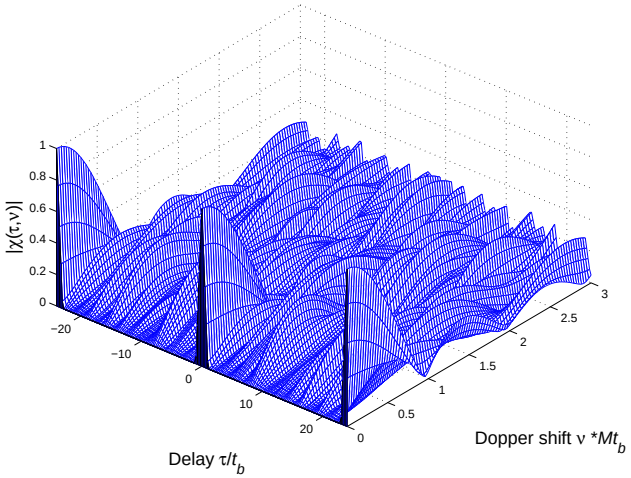

(b)24-length Ipatov codes

Figure 3: Ambiguity function of the code itself: the autocorrelation of the code and its reference code

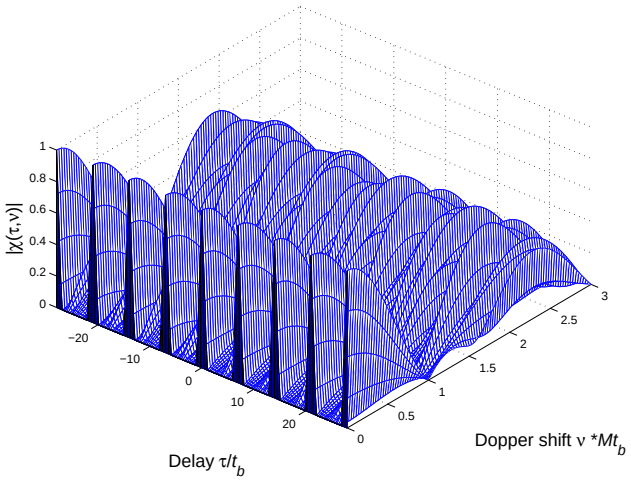

(a)28-length ZCZPS

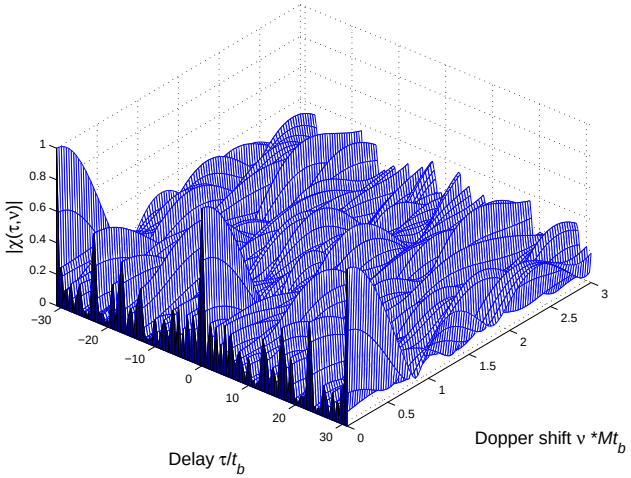

(b)31-length Gold codes

Figure 4: Ambiguity function of radar i (considering interference from radar j)

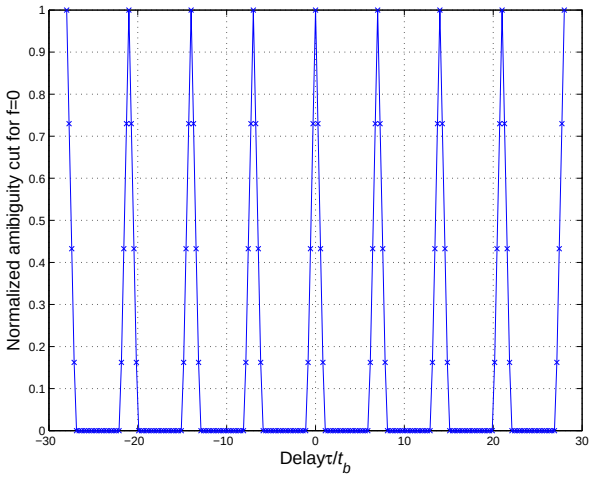

(a)28-length ZCZPS

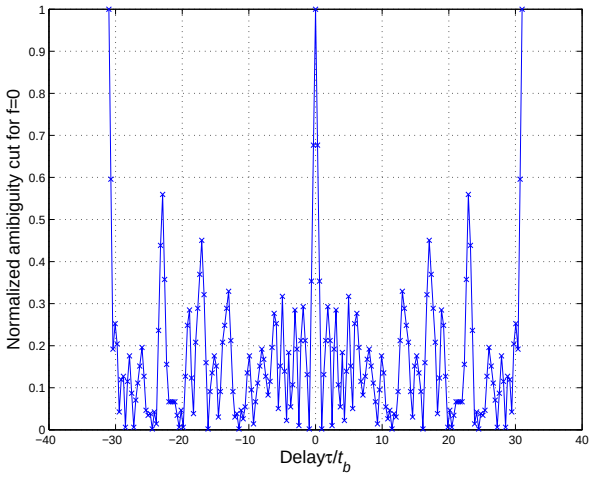

(b)31-length Gold codes

Figure 5: Output of matched filter of radar i (considering interference from radar j) with no Doppler shift

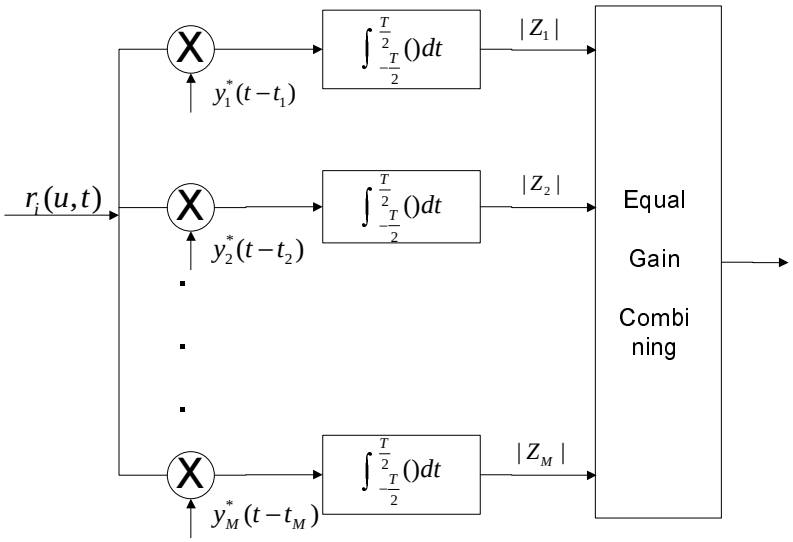

Figure 6: Waveform diversity combining in RSN

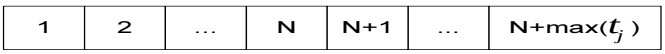

Figure 7: Received Signal Frame

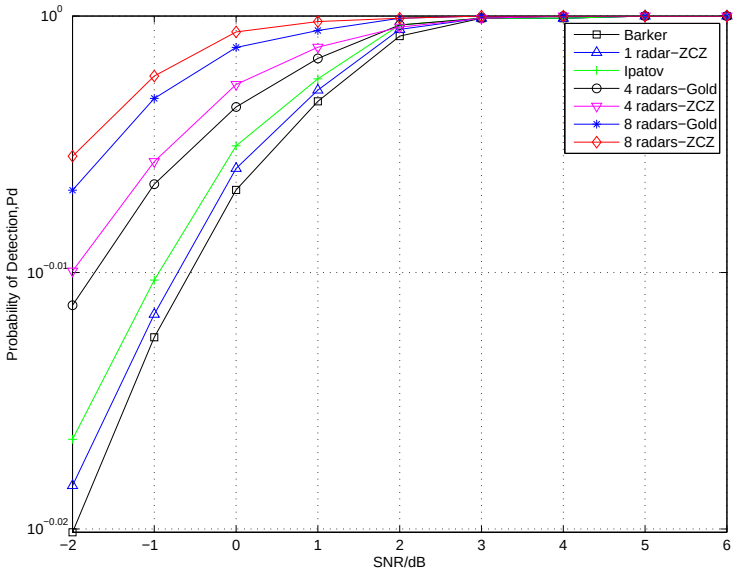

(a) P_D

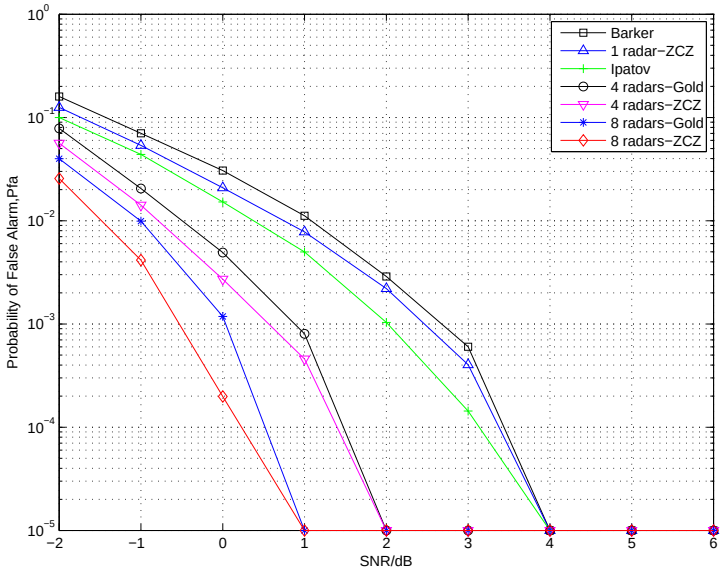

(b)P_{FA}

Figure 8: Under the condition that multiple radar sensors transmit signal synchronously and the target is immovable.

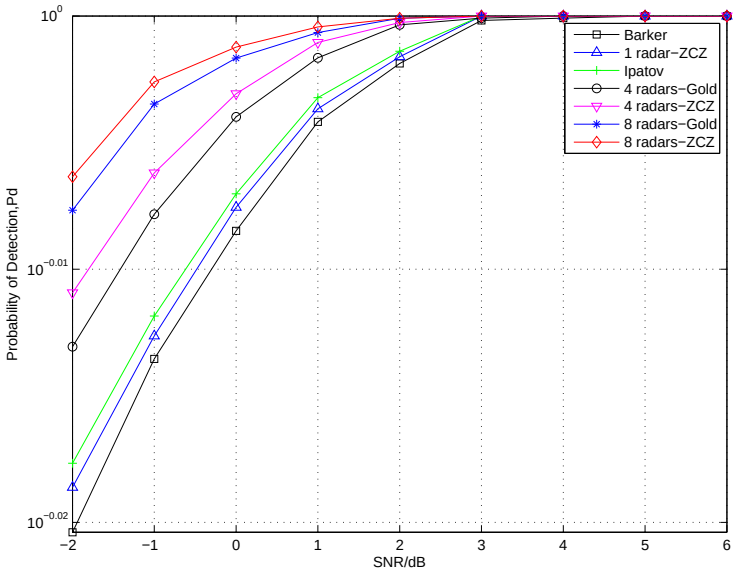

(a)P_D

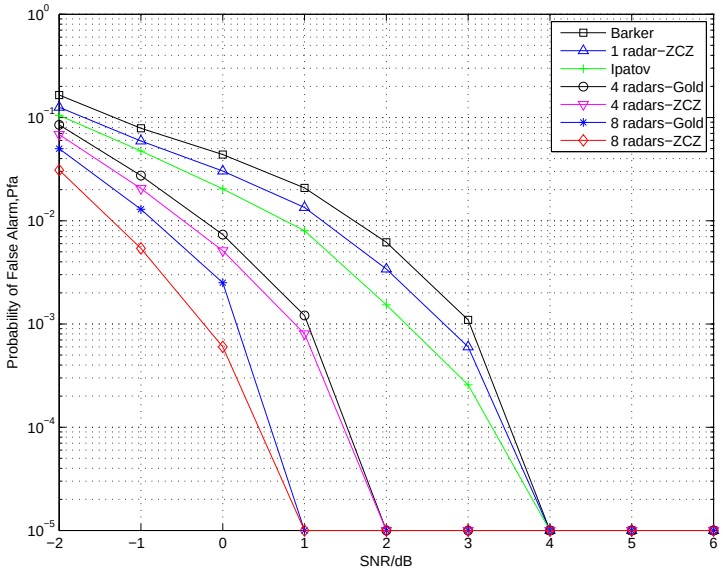

(b)

Figure 9: Under the condition that multiple radar sensors transmit signal synchronously and the target is moving.

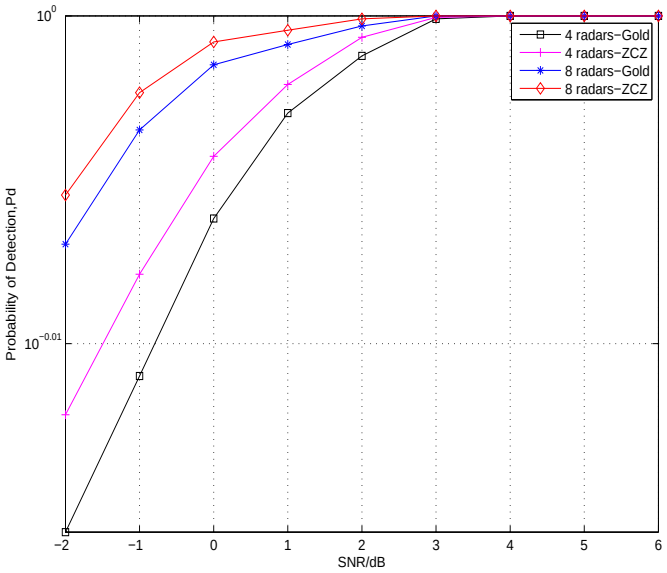

(a)P_D

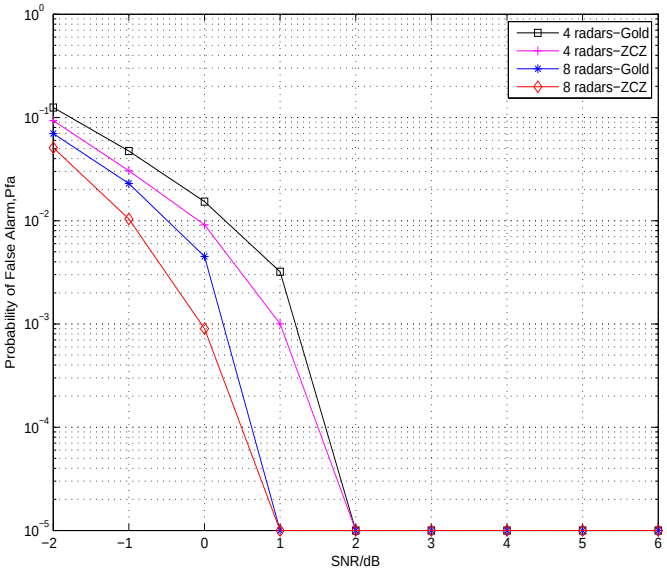

(b)P_{FA}

Figure 10: Under the condition that multiple radar sensors transmit signal asynchronously and the target is moving.